Supporting information

Self assembled fluorosome-polydopamine complex for efficient tumor targeting and commingled photo-dynamic/thermal therapy of triple-negative breast cancer

Rajalakshmi P.S[1,#], Syed Baseeruddin Alvi[1,#], Nazia Begum[2],Bantal Veeresh [2], Aravind Kumar Rengan[1,]*

[1]*Department of Biomedical Engineering, Indian Institute of Technology Hyderabad, Telangana, India, 502285.*

[2]*Department of Pharmacology, G. Pulla Reddy College of Pharmacy, Hyderabad, Telangana, India, 500028.*

[#] Authors contributed equally, *Corresponding Author

Email: aravind@bme.iith.ac.in

Figures

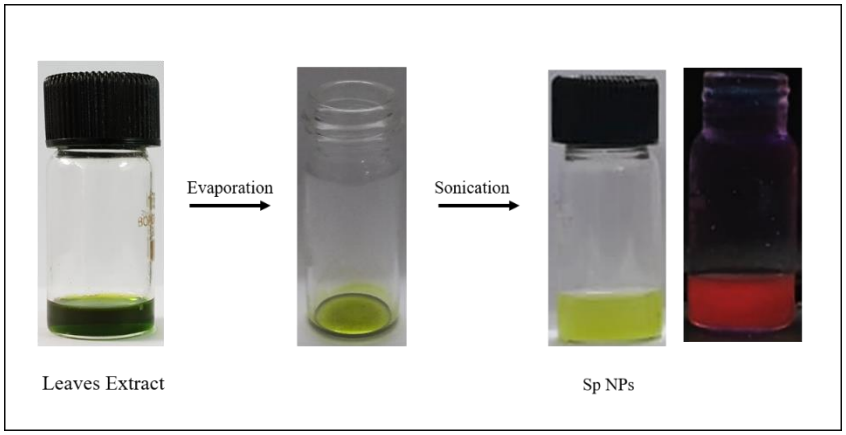

Figure S1: Methodolgy for the preparation of Sp NPs and the fluorescent image of the sample when excited with 365nm UV lamp.

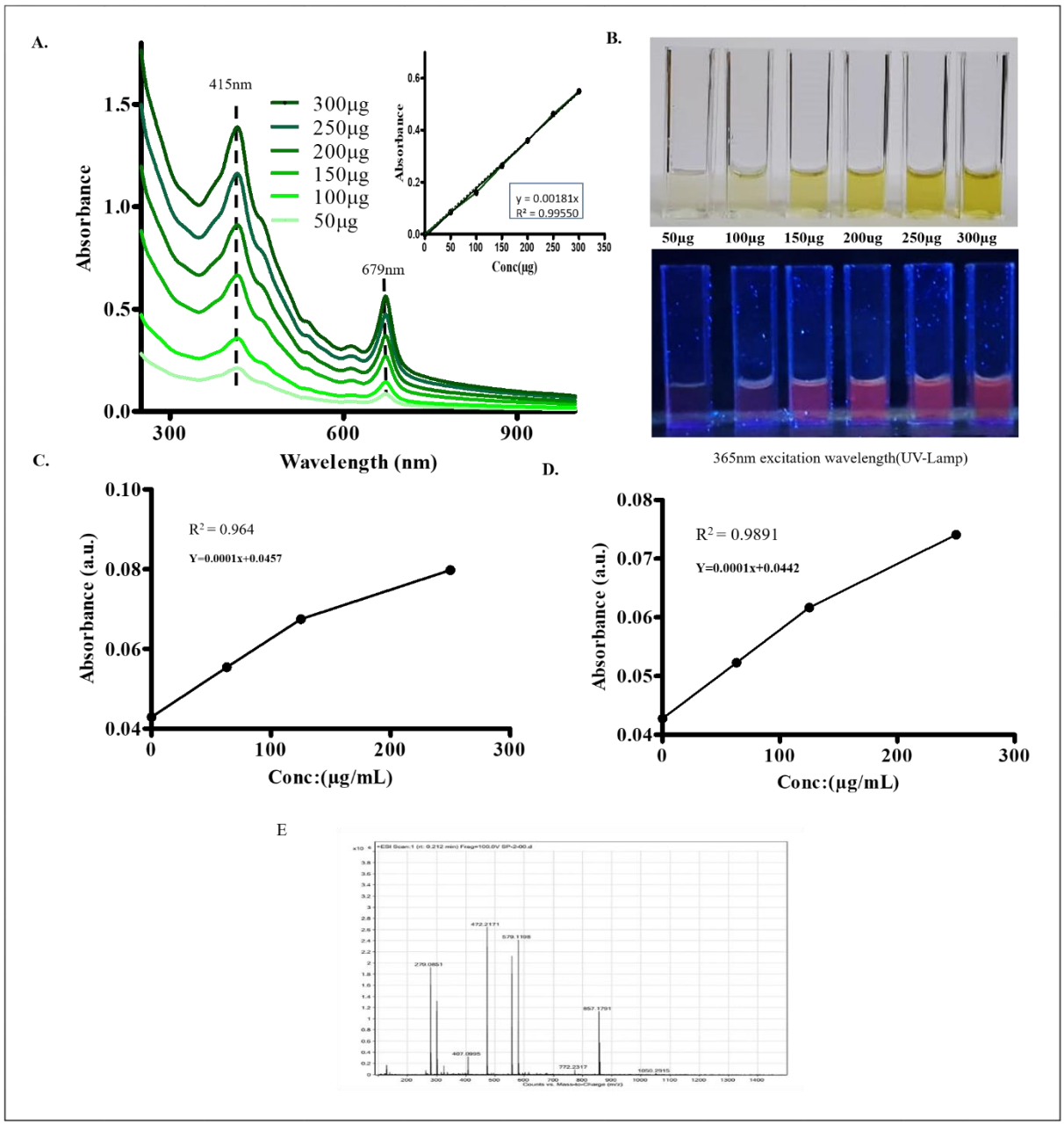

Figure S2: (A**)** Characterization of the Sp NPs by using UV-Vis Spectroscopy and the concentration dependent increase of absorbance. (B) Photograph of the cuvettes containing Sp NPs under normal light and UV light (excitation wavelength: 365nm). (C&D) The quatification of lipid in Sp NPs by taking HSPC as standard. (E) represents the HRMS data of Sp NPs.

HR-MS analysis of the lipid membrane derived from spinach leaves. It has been reported that the lipids present in spinach leaves are abundant in polyunsaturated fatty acids, as shown in **Figure S2 E**. The components having mass/charge ratio in the range of 278 was identified as α linolinic acid (95% of unsaturated fatty acids).[1] The components having mass/charge ratio in the range of 550 to 610 are chlorophyll derivatives.[2,3] The components having mass/charge ratio in the range of 772 was identified as phosphatidylglycerol[4]. These lipids are known to be present in higher proportion in the chloroplast of the plant cell and can self-assemble to form stable structure.

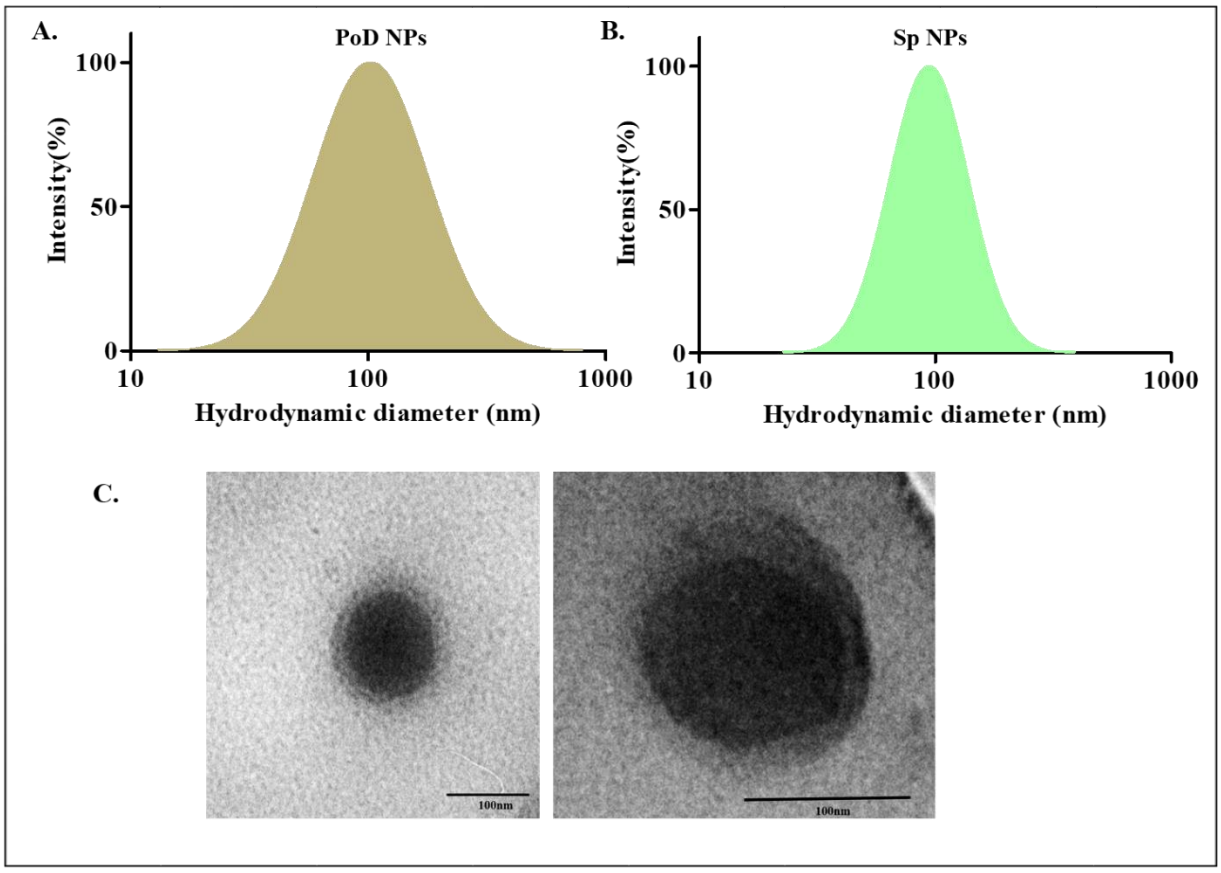

Figure S3: (A&B) Size analysis of PoD NPs and Sp NPs using Particle Sizing (DLS) and (C) TEM images of SPoD NPs.

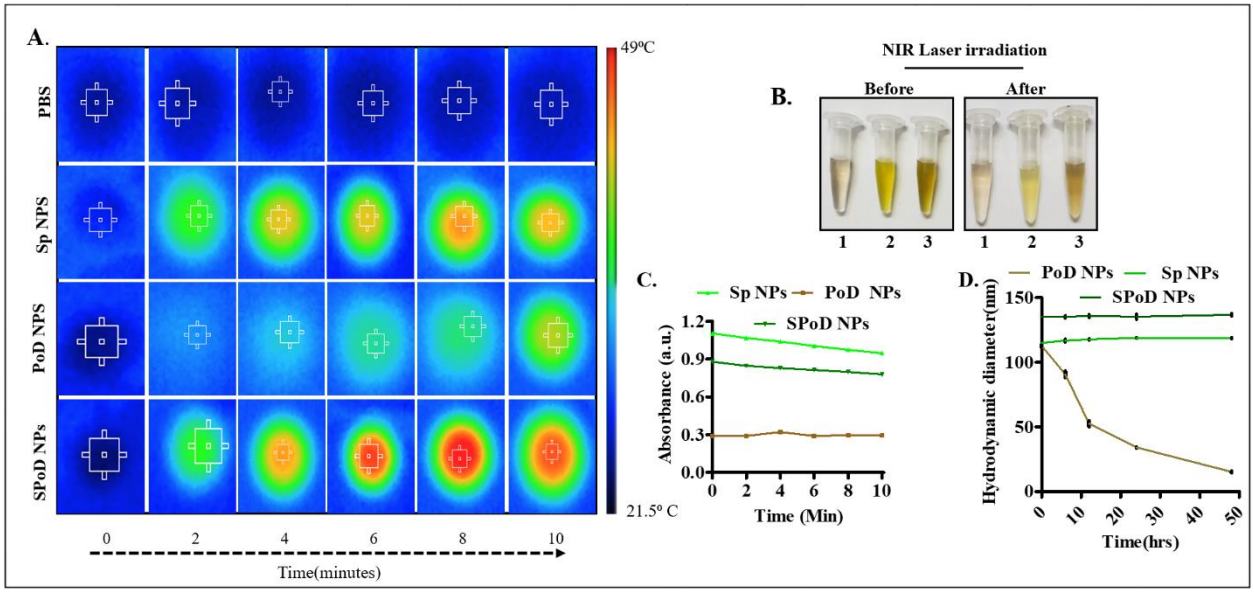

Figure S4: Photothermal transduction efficiency and the stability of PBS, Sp NPs, PoD NPs & SPoD NPs. (A) Thermal images after irradiating with 690nm laser for 10 minutes, (B&C) represents the degradation of PoD NPs, Sp NPs & SPoD NPs upon laser irradiation . (D) represents the serum stability of PoD NPs, Sp NPs & SPoD NPs using Particle sizing.

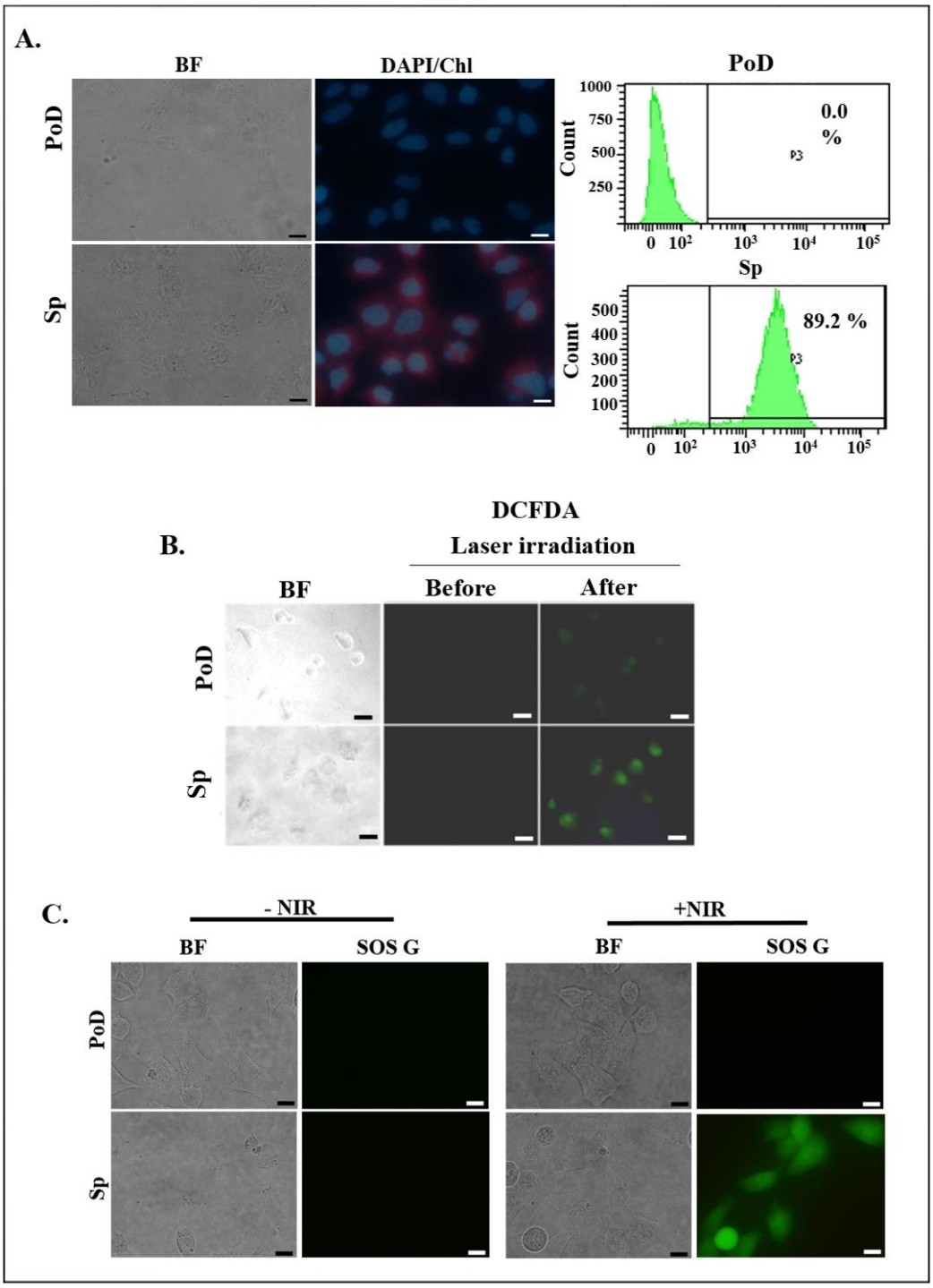

Figure S5: *In vitro* intracellular uptake and the NIR laser mediated intracellular ROS generation. (A) Fluorescence images showing intracellular uptake of the PoD & Sp NPs (DAPI: nuclear stain) (scale bar 20µm) and quantification of the intracellular uptake of the SPoD NPs using flow cytometry. (B) *In vitro* intracellular uptake and the NIR laser mediated intracellular ROS generation by DCFDA in PoD & Sp NPs(scale bar 100µm). (C) NIR laser mediated intracellular generation of Singlet oxygen species by using specific SOS G probe(scale bar 20µm).

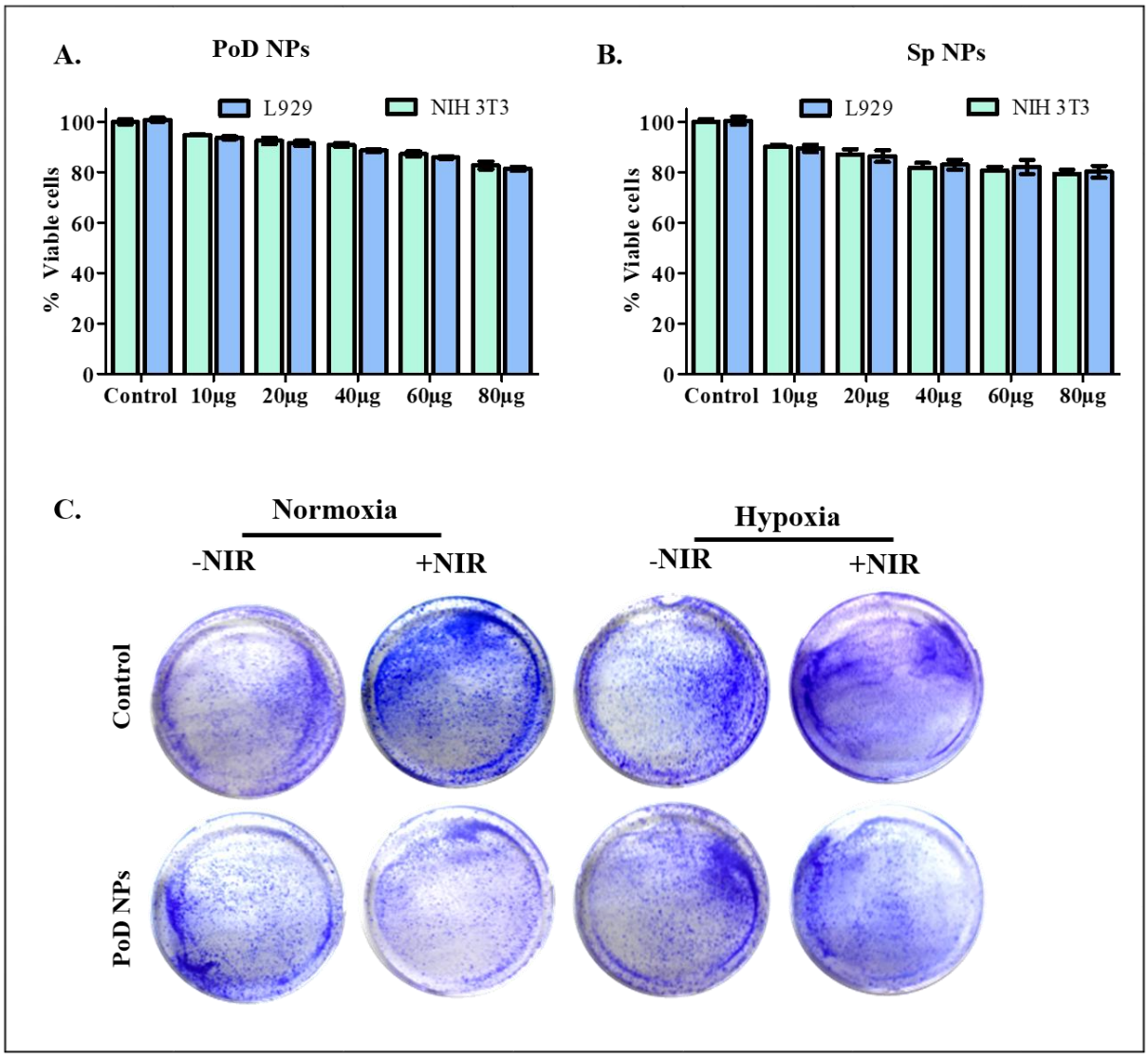

Figure S6: (A&B) shows the biocompactibility of the PoD NPs, Sp NPs in L929 and NIH 3T3 for 48hrs. (C) Clonogenic assay for control and PoD NPs in normoxia and hypoxia.

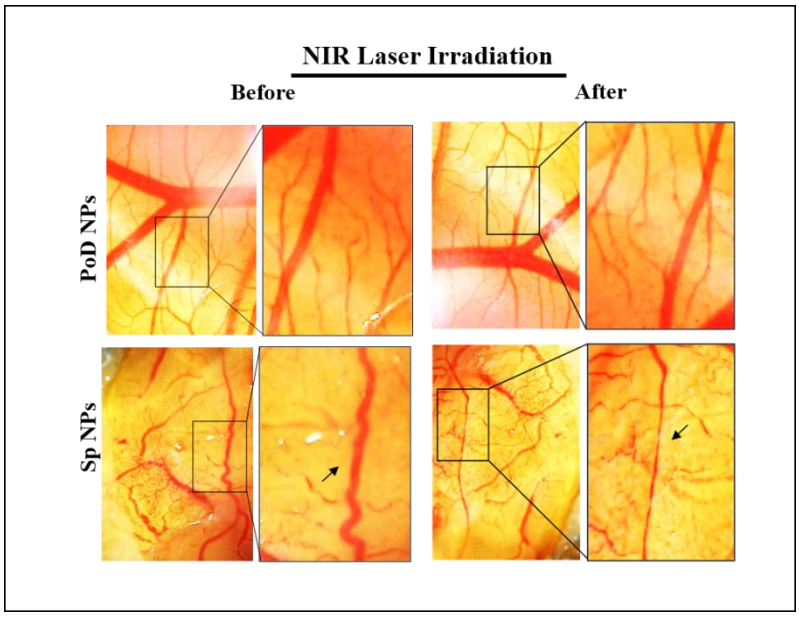

Figure S7: *In ovo* NIR laser mediated vascular disruption by the PoD NPs (PTT) and Sp NPs (PDT).

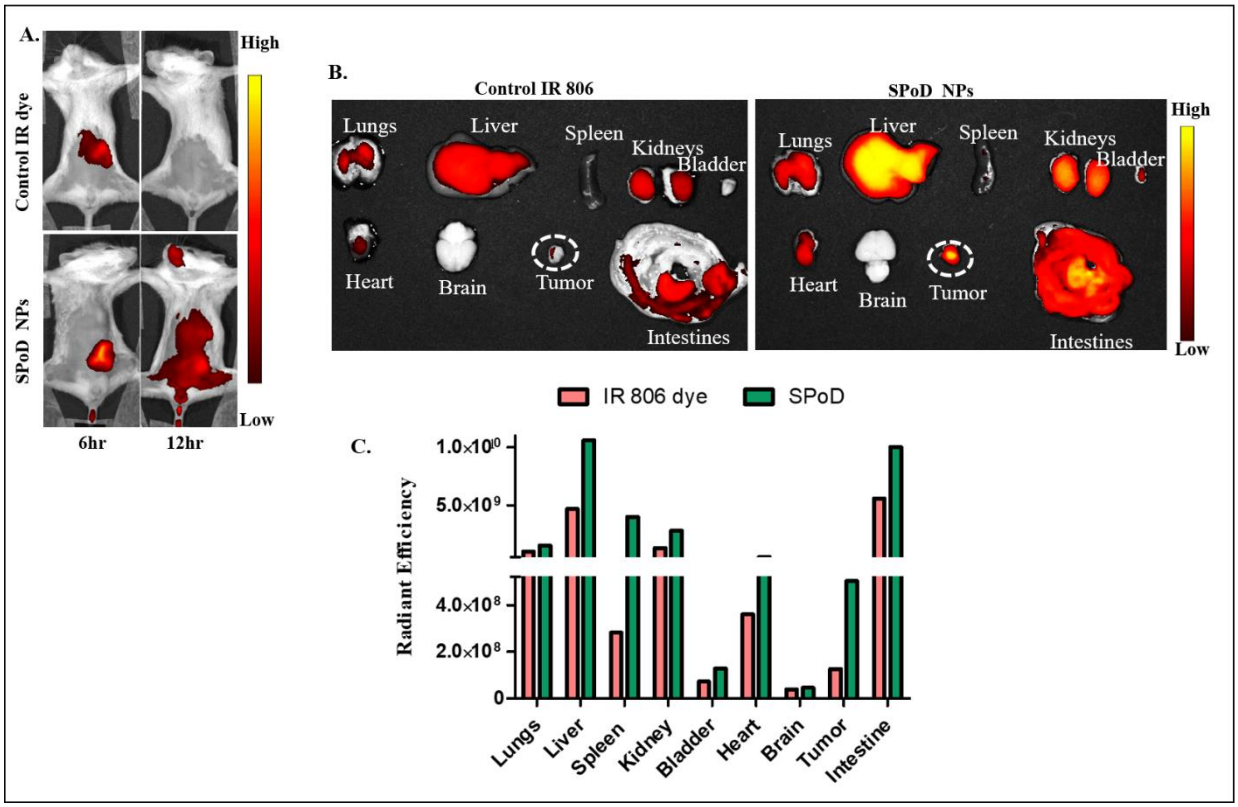

Figure S 8: (A) *In vivo* passive targeting of tumor bycontrol IR 806, SPoD IR NPs evaluated using *in vivo* fluorescent imaging system, (B) the *ex vivo* imaging of control IR806, & SPoD NPs. (C) Graphical representation of biodistribution of the control IR806, & SPoD NPs.

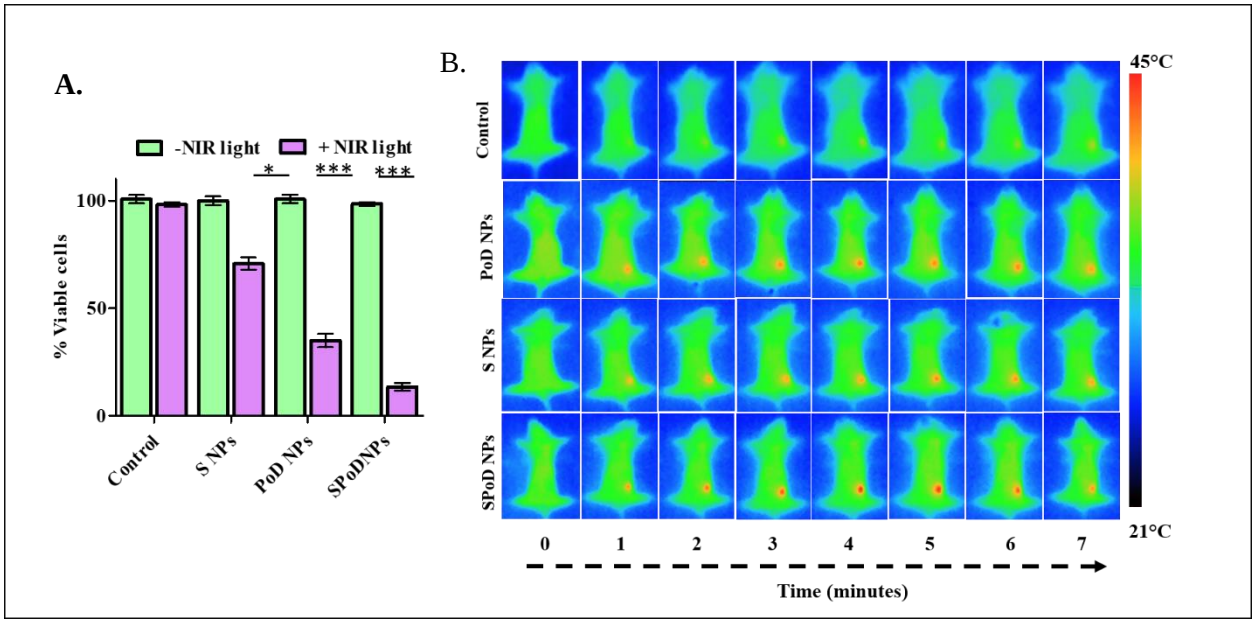

Figure S9: (A) Laser mediated cytotoxicity in 4T1 cell lines and (B) *In vivo th*ermal imaging

Figure S10: *Ex vivo* images of spleen

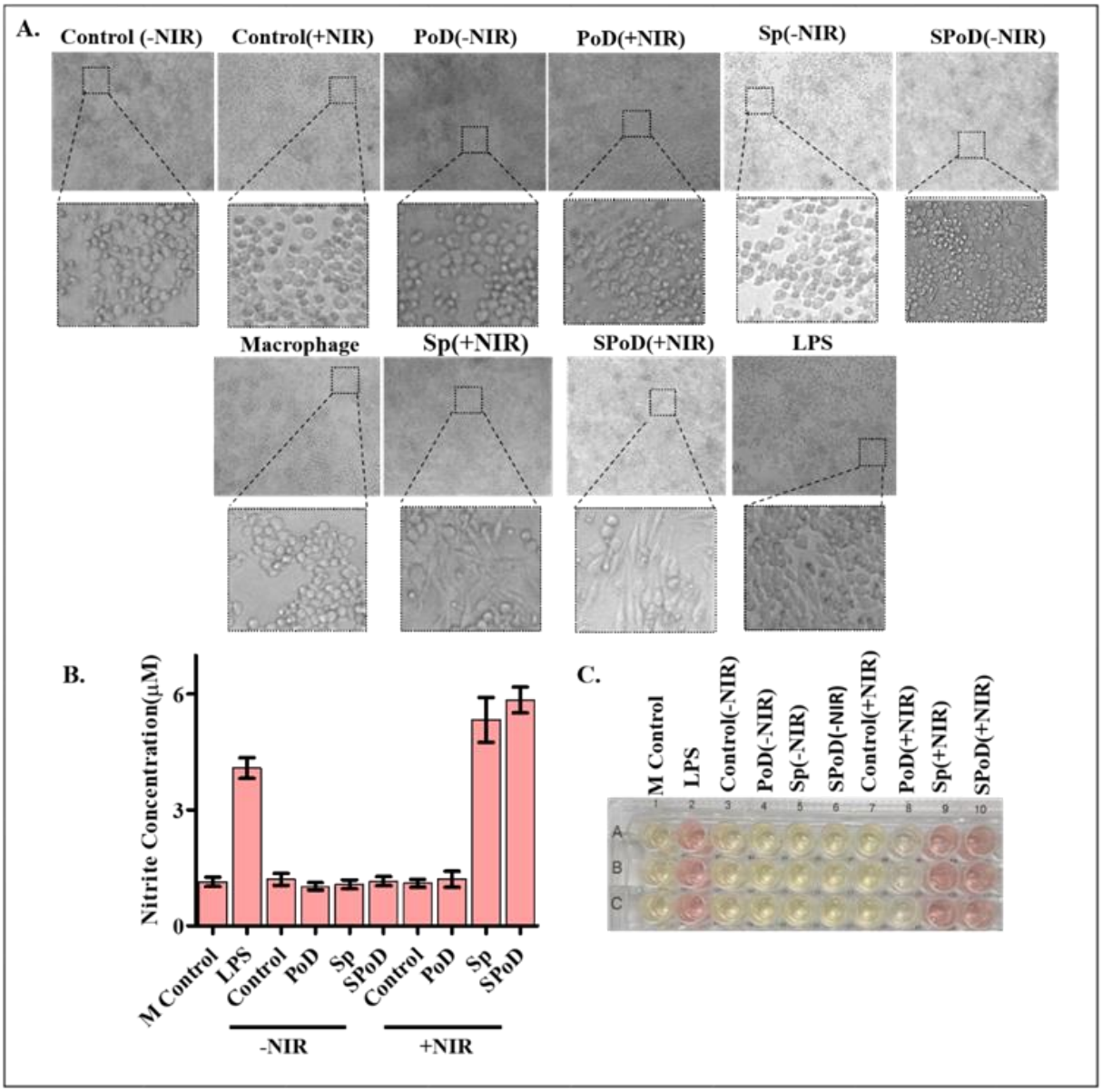

Figure S11:(A)The morphological changes in the monocyte-macrophage cell line (Raw264) after treating it with the NIR irradiated supernatant of the cancer cell. (B & C) represents the Nitrite concentration produced by the monocyte-macrophage cell line (Raw264.1) due to the activation of the cells.

References

1. Wang, R.; Furumoto, T.; Motoyama, K.; Okazaki, K.; Kondo, A.; Fukui, H. Possible Antitumor Promoters in Spinacia Oleracea (Spinach) and Comparison of Their Contents among Cultivars. *Biosci. Biotechnol. Biochem.* **2002**, *66* (2), 248–254. https://doi.org/10.1271/bbb.66.248.

2. (9) van Breemen, R. B.; Canjura, F. L.; Schwartz, S. J. Identification of Chlorophyll Derivatives by Mass Spectrometry. *J. Agric. Food Chem.* **1991**, *39* (8), 1452–1456. https://doi.org/10.1021/jf00008a018.

3. (10) Chen, K.; Ríos, J. J.; Pérez-Gálvez, A.; Roca, M. Comprehensive Chlorophyll Composition in the Main Edible Seaweeds. *Food Chem.* **2017**, *228* (August), 625–633. https://doi.org/10.1016/j.foodchem.2017.02.036.

4. (11) Bei, Y. 乳鼠心肌提取 HHS Public Access. *Physiol. Behav.* **2017**, *176* (3), 139–148. https://doi.org/10.1016/j.ijms.2014.08.026.Ion.